Atti Soc. Tosc. Sci. Nat., Mem., Serie A, **93** (1986)
pagg. 71-85, figg. 6, tabb. 3

G. Berti (**), R. Carrara (*),
L. Leoni (**), M. Saitta (**)

PEAK SHAPE STUDY IN X-RAY POWDER DIFFRACTOMETRY

Riassunto — *Studio dei profili dei picchi in diffrattometria di polvere a raggi-X.* I profili di diffrazione di alcuni riflessi del silicio metallico (radiazione Cu K_β) raccolti con un diffrattometro di polvere, sono stati rappresentati utilizzando tre diversi modelli matematici: (a) somma di tre Lorentziane; (b) somma di una Gaussiana e due esponenziali; (c) somma di una Gaussiana e due Lorentziane.

Nella regione angolare compresa tra 20° e 100° (2 Θ) ed in particolare per valori angolari < 50° il modello (b) sembra essere più adatto a rappresentare il profilo di un picco di diffrazione. Il modello (b) è stato usato per rappresentare i profili dei riflessi di altre sostanze cristalline come galena, fluorite, e quarzo con diverse granulometrie.

Per quarzo, fluorite e silicio, nell'intervallo 20° ÷ 100° (2 Θ) i valori di FWHM (larghezza a metà altezza dei picchi) variano linearmente con la tangente dell'angolo di Bragg; tra queste sostanze il silicio è quella che presenta un minore incremento dei valori di FWHM all'aumentare dell'angolo di Bragg.

I valori di FWHM per i picchi del quarzo con differente granulometria mostrano sistematici incrementi per granulometrie < 2 μ.

Abstract — Silicon Cu K_β X-ray powder diffraction profiles have been represented using three different analytical models: (a) sum of three Lorentzians; (b) sum of a Gaussian and two exponentials; (c) sum of a Gaussian and two Lorentzians.

Model (b), mathematically less simple, seems to be more accurate than the other ones for peak profiles representation, particularly at 2 Θ < 50°. Model (b) was also used to represent peak profiles of fluorite, galena and quartz of different granulometry.

For quartz, fluorite and silicon the peak FWHM (full width at half maximum) values calculated using the model (b) change linearly with the tg Θ (the Bragg angle); among these substances, silicon shows a minor increase of FWHM values.

Peak FWHM values for quartz of different granulometry show small but systematic broadening effects for grain size < 2 μ.

Key words — X-rays powder diffractometry, Cu K_β peak profiles, FWHM - Bragg's angle relationship.

(*) Dipartimento di Fisica - Università di Pisa - Piazza Torricelli 2 - 56100 Pisa.
(**) Dipartimento Scienze della Terra - Università di Pisa - Via S. Maria 53 - 56100 Pisa.

Introduction

The single Lorentzian or Gaussian is generally not recognized to be an adequate analytical description of the peak shape in X-ray powder diffractometry. Malmros and Thomas (1977) and Young *et al.* (1977) showed that the peak profile may be approximated by a modified Lorenz function. Cattax and Cox (1977) introduced an intermediate Lorentz function to represent silicon Cu K_β reflections. Satisfactory analytical descriptions of line profile shape were also obtained by the convolution of suitable functions (Klug and Alexander, 1974) or more simply overlapping several Lorentzians (Taupin, 1973; Parrish *et al.*, 1983), Gaussian and two exponentials (Berti *et al.*, 1984). This paper reports on the representation, using a personal computer program, of the 111, 220, 311, 400, 422 and 531 Cu K_β peak profiles of silicon according to three different mathematical models: a) sum of three Lorentzians; b) sum of a Gaussian and two exponentials; c) sum of a Gaussian and two Lorentzians. Model b) was used to represent Cu K_β peak profiles of other crystalline substances: fluorite (111, 220, 311, 422, 531 reflections), quartz (101, 112, 213 reflections) and galena (111, 200, 311, 422 reflections). The relationship between the Bragg angle and the FWHM (full width at half maximum) of quartz, silicon and fluorite peaks and also the dependence of FWHM on the powder grain size (for quartz samples) were investigated.

Specimen preparations

Crystal fragments of quartz, fluorite, galena and powdered silicon (BDH silicon of the British Drug House Ltd Chemical Division) were used. Each sample was placed in the agata mortar and hand-ground with an agata pestle until final traces of grittiness had disappeared. Powder samples with granulometry $< 10\ \mu$ were selected for silicon, quartz and fluorite by decanting the powder in distilled water; for quartz, powder samples with granulometry $< 32\ \mu$, $< 16\ \mu$ and $< 2\ \mu$ were also selected.

No granulometric control was performed on the galena sample; galena was chosen because it underwent mechanical deformations on grounding which may be partially readsorbed by heating. This made it possible to verify the proposed mathematical representa-

tions also on peaks more or less affected by lattice distortion broadening.

Measurement operating conditions

The diffraction peak intensities were measured by a PW 1730 Philips automatic X-ray diffractometer on line with an Olivetti P 6066 personal computer which was also used for data processing. The diffractometer was equipped with a graphite AMR 3-202 GVW 7038 focusing monochromator. The operating conditions during the measurements were as follows:

— broad focus Cu X-ray tube supplied by 40 KV-20 mA; K_β radiation

— take-off angle 6° with a focal spot dimension of 0.2 x 12 mm

— divergence and scatter slits 1° and 4° wide in the 2 Θ region 18° ÷ 74° and > 74° respectively; the geometry of the diffractometer includes Soller slits

— focusing slit 0.02 mm wide.

Each reflection was collected sampling 2.00° (2 Θ) wide range with a scanning step of 0.02°. The counting time was chosen in such a way as to have a statistical counting error smaller than 2.5% on the maximum of each peak.

Peak-profile functions

Three different representations were used to represent mathematically the peak profiles:

a) Sum of three Lorentzian curves (3 L representation)

$$Y(2\Theta) = \sum_{1}^{3}{}_i \frac{I_i \sigma_i^2}{\sigma_i^2 + (2\Theta - 2\Theta_i)^2} + B \qquad (1)$$

where I_i, σ_i and $2\Theta_i$ are the maximum intensity value, the half width at half maximum and the angular position respectively of the «..iesima» lorentzian.

b) Sum of a Gaussian and exponential curves (G2E representation)

$$Y(2\Theta) = I_G\, e^{-(2\Theta-2\Theta_G)^2/d^2} + Ie^{-b|2\Theta-h|} + B \qquad (2)$$

I_G, d and $2\Theta_G$ are the maximum intensity value, half width at half maximum and the peak position of the gaussian; I and h represents the maximum value of the exponential curves and their position respectively. Equation 2 differs from that proposed by BERTI *et al.* (1984) since the exponentials are cut at 2Θ value of the maximum of the gaussian function.

c) Sum of a gaussian and two lorentzian curves (G2L representation).

$$Y(2\Theta = I_G\, e^{-(2\Theta-2\Theta_G)^2/d^2} + \sum_1^2{}_i \frac{I_i\, \sigma_i^2}{\sigma_i^2 + (2\Theta - 2\Theta_i)^2} + B \qquad (3)$$

Symbols as in equations (1) and (2).

For each representation the nine parameters were calculated by a best fitting procedure minimizing the function:

$$\chi^2 = \sum_{i=1}^{n} W_i[Y(2\Theta_i)_o - Y(2\Theta_i)_c]^2$$

where $Y(2\Theta_i)_o$ and $Y(2\Theta_i)_c$ are the observed and calculated intensity values respectively, $W_i = 1/Y(2\Theta_i)_o$ the statistic weight associated with each observed intensity value and n the measured points number.

The background B was measured at $\pm 1°$ from the maximum of each peak and linearly interpolated in this range. Figures 1 (a, b, c), 2 (a, b, c) and 3 (a, b, c) show the 111, 311 and 531 peak profiles of silicon respectively (in each figure the labels a, b and c mark in order the model (3L), (G2E) and (G2L)); the functions used to describe the peak profiles together with the observed and calculated line profiles are also sketched. Table 1 lists the parameter values for each model adjusted by the least square fit procedure.

In Table 2, for the silicon 111, 220, 311, 400, 422 and 531 reflections the maximum intensity, the 2Θ position of the maximum and the FWHF values resulting from the calculated diffraction profiles are given.

Figures 1, 2, 3 and the parameter values reported in table 1 show that the proposed mathematical representations are equivalent;

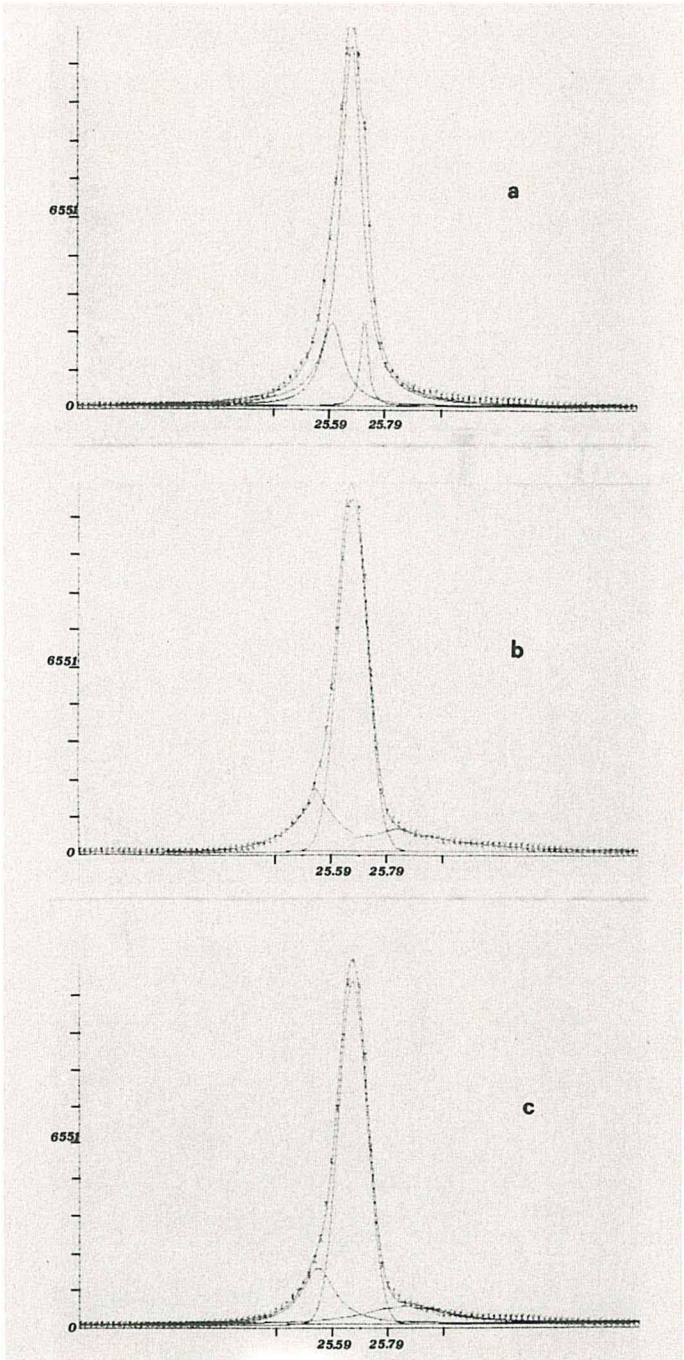

Fig. 1 - Silicon 111 reflection; observed (crosses) and calculated (continue lines) peak profile together with the pure utilized functions. (a), (b) and (c) pictures refer to (3L), (G2E) and (G2L) representations respectively.

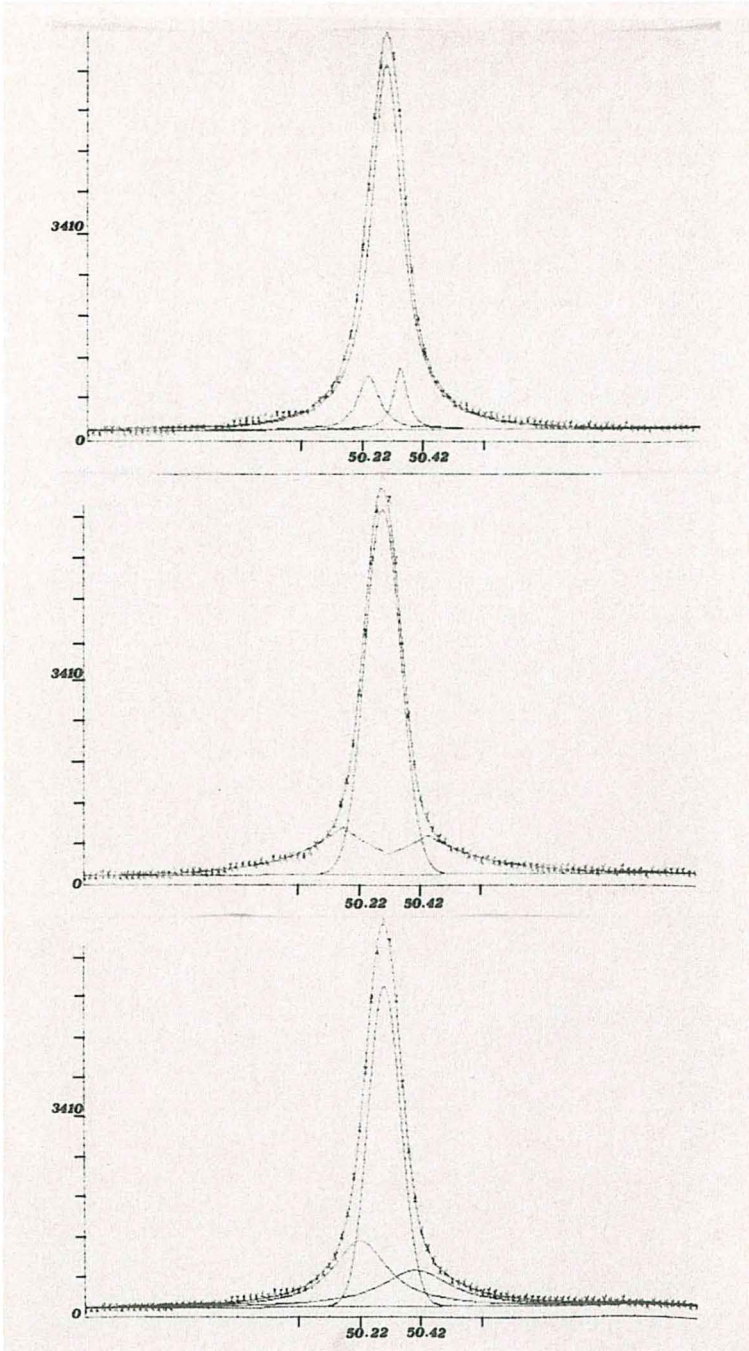

Fig. 2 - Silicon 311 reflection; observed (crosses) and calculated (continue lines) peak profile together with the pure utilized functions. (a), (b) and (c) as in fig. 1.

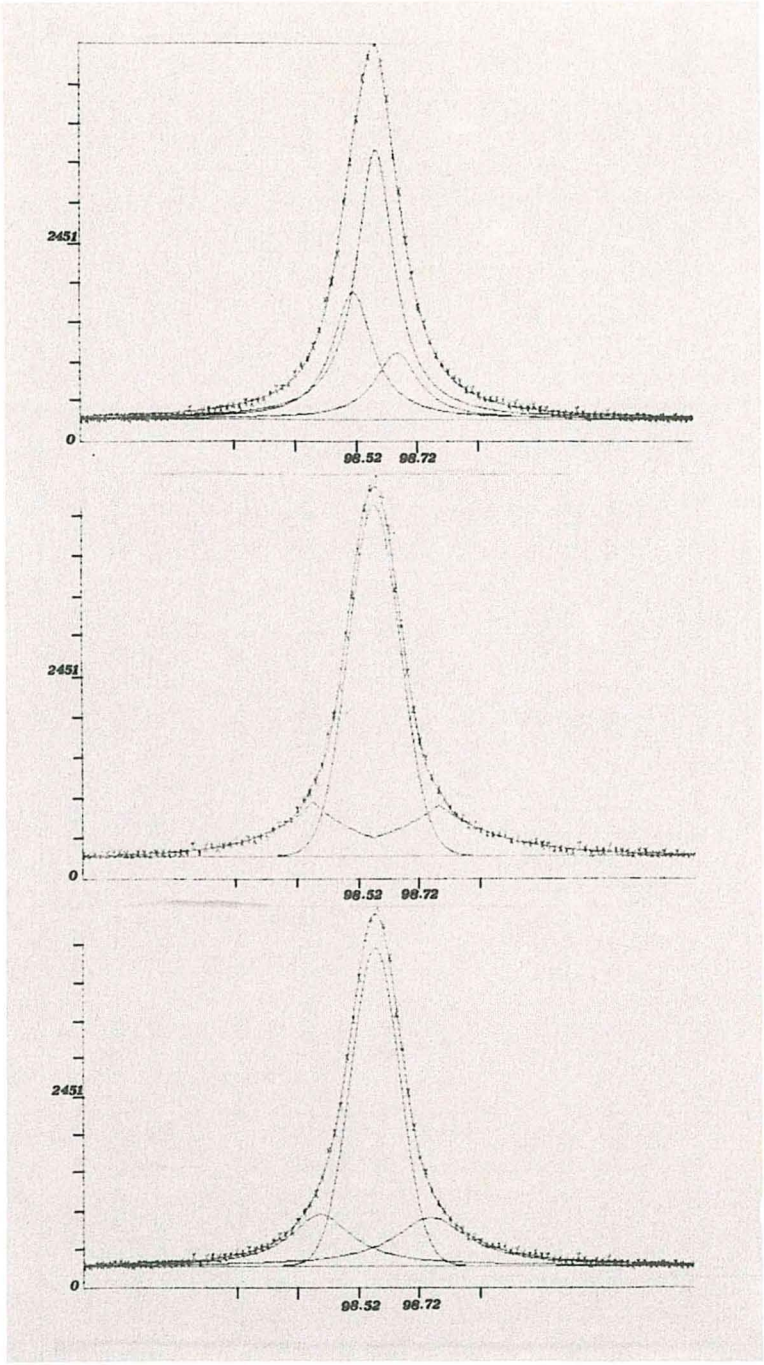

Fig. 3 - Silicon 531 reflection; observed (crosses) and calculated (continue lines) peak profile together with the pure utilized functions. (a), (b) and (c) as in fig. 1.

TABLE 1 - Parameter values of the (G2E), (G2L) and (3L) peak functions. Silicon 111, 311 and 531 reflections.

(G2E)

	I_G	$2\Theta_G$	σ_G	I_L	2Θ	b_L	I_R	2Θ	b_R	F_1	F_2	χ^2
111	12354	25.665	5.20	2174	25.540	.095	827	25.824	.0390	100	150	383
311	5998	50.298	580	802	50.168	.056	550	61.821	.045	250	300	153
531	4259	98.573	8.43	662	98.372	.058	624	98.782	.050	280	280	123

(G2L)

	I_G	$2\Theta_G$	σ_G	I_1	$2\Theta_1$	σ_1	I_2	$2\Theta_2$	σ_2			
111	12205	25.666	5.11	1986	25.542	7.11	632	25.852	17.71	»	»	594
311	5791	50.298	5.76	675	50.181	13.58	475	50.443	14.85	»	»	325
531	4100	98.573	7.94	648	98.395	12.23	609	98.757	14.73	»	»	146

(3L)

	I_1	$2\Theta_1$	σ_1	I_2	$2\Theta_2$	σ_2	I_3	$2\Theta_3$	σ_3			
111	12288	25.666	4.48	2856	26.600	5.03	3101	25.715	1.55	»	»	654
311	5920	50.300	6.00	905	50.239	4.06	1025	50.342	2.55	»	»	334
531	3326	98.583	7.38	1564	98.508	7.83	813	98.652	8.66	»	»	227

$\sigma = \frac{d}{1.17}$, values are given as degrees $\times 10^{-2}$; result from 101 fitted experimental points.

TABLE 2 - $2\Theta_{max.}$, $I_{max.}$ and FWHM values of silicon peaks calculated by the three different representations; χ^2 values resulting from 101 fitted experimental points are also given.

	(G2E)				(G2L)				(3L)			
	$2\Theta_{max.}$	$I_{max.}$	FWHM	χ^2	$2\Theta_{max.}$	$I_{max.}$	FWHM	χ^2	$2\Theta_{max.}$	$I_{max.}$	FWHM	χ^2
111	25.664	13019	13.1	383	25.665	13000	13.0	594	25.665	13744	12.5	654
220	42.506	4856	13.6	175	42.507	4595	13.5	327	42.507	4635	13.1	489
311	50.297	6482	14.7	153	50.299	6559	14.4	325	50.300	6648	14.1	334
400	61.637	5317	18.2	153	61.639	5278	18.3	164	61.639	5317	17.6	195
331	67.876	4576	17.8	152	67.877	4429	18.0	190	67.886	4397	17.6	239
422	77.735	4776	17.4	220	77.738	4891	16.8	183	77.736	4930	16.9	195
531	98.574	4479	21.7	123	98.573	4545	21.2	146	98.578	4652	20.9	127

in fact peak profiles may be described in each model by the sum of a symmetric central function (Gaussian or Lorentzian), whose integral is generally more than 70% of the experimental peak area, and two lateral functions representing the peak tails.

At 2 Θ values close to 90° a single Lorentzian function seems to be sufficient to represent peak profiles as shown in Fig. 4 which pictures the silicon 531 peak profile obtained by using a single Lorentzian. This suggests that at 2 Θ near 90° three Lorentz functions (3L model) appear to be redundant; Fig. 3a shows only one of several possible cases.

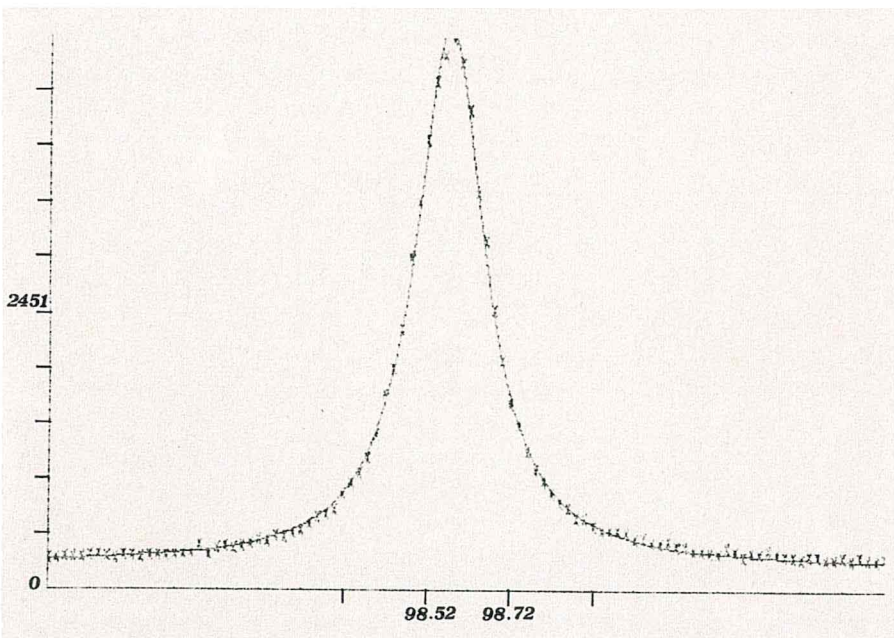

Fig. 4 - Silicon 531 reflection. Peak profile obtained using a single Lorentzian (χ^2 = 190, number of points 101).

The intensity, 2 Θ and FWHM values of the silicon peaks (Table 2) computed according to the three representations prove to be similar; however, a comparison of χ^2 values shows that model G2E is more satisfactory than the others, particularly at low values of 2 Θ (< 50°).

Model G2E was used to represent the peak profiles of some

TABLE 3 - $2\Theta_{max.}$, $I_{max.}$ and FWHM values of fluorite, galena and quartz peaks calculated by the G2E function.

	$2\Theta_{max.}$	$I_{max.}$	FWHM	χ^2		$2\Theta_{max.}$	$I_{max.}$	FWHM	χ^2
		FLUORITE					QUARTZ (< 2 μ)		
111	25.500	10377	14.54	290	101	24.026	7032	14.28	156
220	42.235	5579	16.72	220	110	32.908	2670	14.80	97
311	49.974	2868	17.91	194	112	45.002	4371	15.62	190
422	77.171	1947	24.88	154			QUARTZ (< 10 μ)		
531	97.743	1076	31.35	114	101	24.020	8516	13.06	165
		GALENA			110	32.898	3850	13.61	135
111	23.426	5196	23.02	177	112	45.001	6250	14.83	222
111*	23.457	5793	18.34	350	212	60.441	1384	17.14	123
200	27.126	13463	15.99	304	114	72.253	1819	18.02	147
200*	27.150	13198	14.43	259			QUARTZ (< 16 μ)		
311	45.769	4651	26.08	214	101	24.018	8659	13.15	162
311*	45.787	5715	19.69	192	110	32.897	3775	12.67	128
422	70.114	1068	39.40	110	112	44.998	6049	13.96	271
422*	70.123	2887	30.26	115			QUARTZ (< 32 μ)		
					101	24.017	8473	12.62	217
					110	32.893	3932	12.91	101
					112	45.000	6382	13.41	350

* After heating at 250°C for 16 h.
χ^2 values result from 101 fitted experimental points.

fluorite quartz and galena reflections too. Table 3 reports the calculated intensity, 2 Θ and FWHF values of such reflections together with the χ^2 values.

Four series of data for quartz are presented; the first series refers to powder samples with a grain size $< 2\ \mu$, the second, third and fourth ones to powder samples with a grain size < 10, < 16 and $< 32\ \mu$ respectively. Fig. 5 (a and b) shows the galena peak profiles before and after heating at 250° C for 16 h.

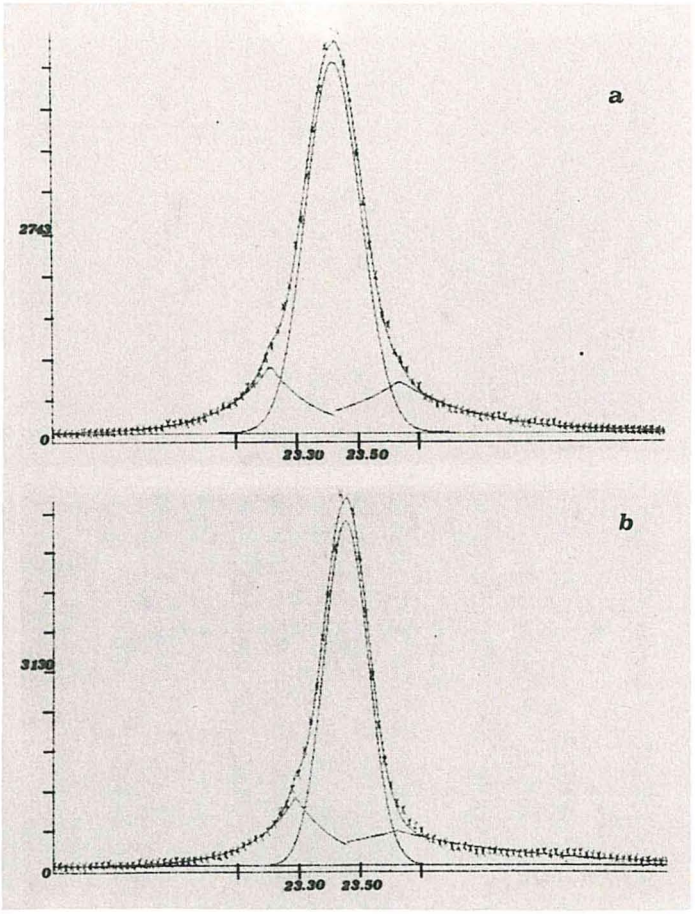

Fig. 5 - Galena 111 reflection. Peak profiles resulting from G2E representation. (a) and (b) pictures refer to galena samples before and after heating the powder at 250° C for 16 h respectively.

FWHM - Bragg's angle relationship

For silicon, quartz and fluorite it turns out that the peak FWHM values calculated using the G2E function in the 2 Θ range of 20° ÷ 100°, are related to Bragg's angle by:

$$FWHM = K + K'tg\Theta$$

For these substances the peak FWHM values against the tgΘ are plotted in Fig. 6; values of K and K' computed by a least square method are also reported; K assume almost the same value for all the studied substances (its value presumably depending on the diffractometry geometry), while the K' value seems to vary decreasing from fluorite to silicon.

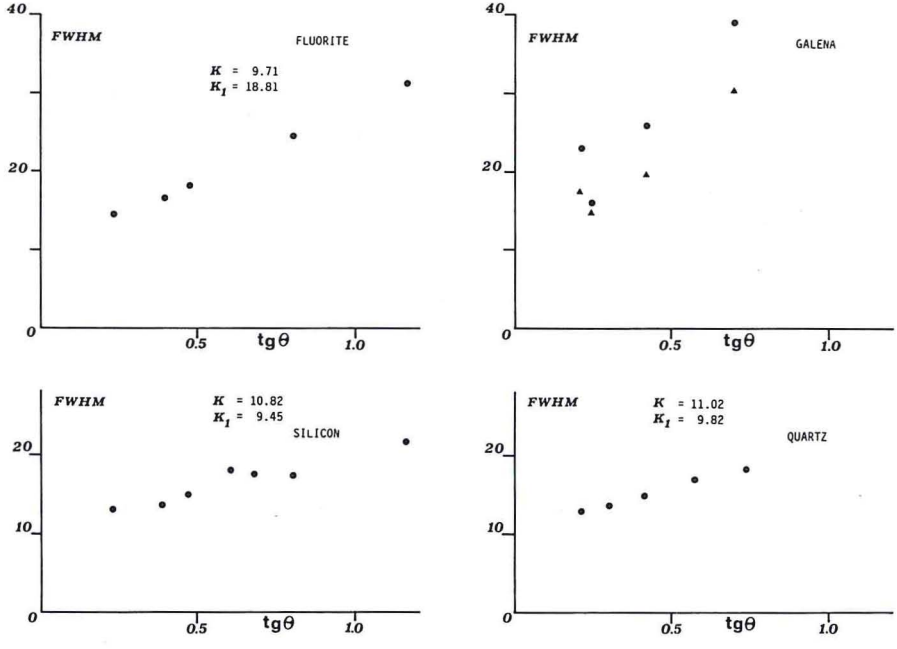

Fig. 6 - FWHM - Bragg's angle relationship.

Owing to the presence of lattice-deformation broadening, peak FWHM values of natural galena show an irregular behaviour; however, after heating, FWHM values tend to change linearly with the Bragg angle for this substance as well.

FWHM values calculated on quartz powders of $< 32\ \mu$ and $< 16\ \mu$ are very similar one to each other and somewhat smaller than those calculated on quartz powder $< 10\ \mu$ and $< 2\ \mu$, the increase of FWHM values being systematic on quartz powder of $< 2\ \mu$.

Thus FWHM of quartz peaks seem to suggest that peak broadening due to grain size effects become observable beginning from powders $< 2 \div 10\ \mu$.

Conclusions

In X-ray powder diffracrometry, peak profiles may be mathematically described with sufficient accuracy as the sum of several functions; for Cu K_β reflections, at least, the sum of three functions (three Lorentzians, a gaussian and two exponentials or a Gaussian and two Lorentzians) in the $2\ \Theta$ range $20° \div 100°$ seem to be sufficient to represent peak profiles. At $2\ \Theta$ values close 90° a satisfactory description of peak profiles may be obtained even by a single lorentzian.

Although at $2\ \Theta < 50°$ the G2E peak functions generally seems more accurate than the other two models, typical quantities of a diffraction peak as maximum intensity, $2\ \Theta$ position and FWHM values calculated through the three proposed models tourn out to be similar. In the $2\ \Theta$ range of 20°-100° the FWHM values of silicon, quartz and fluorite peaks are linearly related to the Bragg's angle trigonometric tangent. The FWHM-tgΘ relationship suggest a method for experimental determination of the instrumental function of a diffractometer. Indeed the peak-shape of crystalline substances whose reflections show small FWHM values (low K' values in the FWHM-tgΘ relationship) may represent a good approximation of the instrumental effects.

As regards the peak broadening due to powder granulometry, the experimental data collected on quartz point out that small but systematic broadening effects are observed for grain size $< 2\ \mu$ and perhaps also for grain size $< 10\ \mu$.

REFERENCES

Berti G., Carrara R., Leoni L. (1984) - A peak analysis method in X-ray powder diffractometry. *Rend. Soc. It. Min. e Petrol.*, **39** (1), 115-122.

KLUG H.P., ALEXANDER L.E. (1974) - X-ray diffraction procedures for policrystalline and amorphous materials. Ed. J. Wiley & Sons, New York.

KATTAK C.P., COX D.E. (1977) - Profile analysis of X-ray powder diffractometer data: structural refinement of $La_{0.75}$ $Sr_{0.25}$ CrO_3. *J. Appl. Cryst.*, **10**, 405-411.

MALMROS G., THOMAS J.O. (1977) - Least-square structure refinement based on profile analysis of powder film intensity data measured on an automatic microdensitometer. *J. Appl. Cryst.*, **10**, 7-11.

TAUPIN D. (1973) - Automatic peak determination in X-ray powder patterns. *J. Appl. Cryst.*, **6**, 266-273.

WILL G., PARRISH W., HUANG T. (1983) - Crystal structure refinement by profile fitting and least square analysis of powder diffractometer data. *J. Appl. Cryst.*, **16**, 611-622.

YOUNG R.A. (1980) - Structural analysis from X-ray powder diffraction patterns with the Rietveld method. *N.B.S. Sp-c*, Pub., **567**, 143-163.

(ms. pres. il 31 luglio 1986; ult. bozze il 30 marzo 1987)